

UNCLASSIFIED

AD NUMBER

AD883334

LIMITATION CHANGES

TO:

Approved for public release; distribution is unlimited.

FROM:

Distribution: Further dissemination only as directed by Air Force Cambridge Research Labs., Hanscom AFB, MA, MAY 1971, or higher DoD authority.

AUTHORITY

AFCRL ltr 1 Dec 1976

THIS PAGE IS UNCLASSIFIED

AEDC-TR-71-72

cy5

AEDC-OI 7-7-103

MAY 19 1971  
MAY 21 1971  
MAY 24 1971  
JUN 18 1971  
FEB 9 1982



## FINAL PREFLIGHT CALIBRATION OF ARPA/AFCRL CVF II SPECTROMETER

14 JUN 1977

APPROVED FOR RELEASE

ARNOLD OFFICE OF INFORMATION  
ARNOLD ENGINEERING DEVELOPMENT CENTER  
ARNOLD AIR FORCE STATION, TENN. A32389  
ARO, Inc.

and

T. P. Condron

USAF

May 1971

This document has been approved for public release  
and its distribution is unlimited.

This document may be further distributed by any holder  
only with specific prior approval of Air Force  
Cambridge Research Laboratories (CROL), L. G.  
Hanscom Field, Bedford, Massachusetts 01730.

**VON KÁRMÁN GAS DYNAMICS FACILITY  
ARNOLD ENGINEERING DEVELOPMENT CENTER  
AIR FORCE SYSTEMS COMMAND  
ARNOLD AIR FORCE STATION, TENNESSEE**

# ***NOTICES***

When U. S. Government drawings specifications, or other data are used for any purpose other than a definitely related Government procurement operation, the Government thereby incurs no responsibility nor any obligation whatsoever, and the fact that the Government may have formulated, furnished, or in any way supplied the said drawings, specifications, or other data, is not to be regarded by implication or otherwise, or in any manner licensing the holder or any other person or corporation, or conveying any rights or permission to manufacture, use, or sell any patented invention that may in any way be related thereto.

Qualified users may obtain copies of this report from the Defense Documentation Center.

References to named commercial products in this report are not to be considered in any sense as an endorsement of the product by the United States Air Force or the Government.

FINAL PREFLIGHT CALIBRATION OF  
ARPA/AFCRL CVF II SPECTROMETER

F. Arnold

ARO, Inc.

and

T. P. Condron

USAF

~~This document may be further distributed by any holder  
only with specific prior approval of Air Force  
Cambridge Research Laboratories (CRRL), L. G.  
Hanscom Field, Bedford, Massachusetts 01730.~~

## FOREWORD

The work reported herein was sponsored by Air Force Cambridge Research Laboratories (AFCRL) (CROR), Bedford, Massachusetts, under System 920F, Program Element 62301D, Project 0450.

The results presented were obtained by ARO, Inc. (a subsidiary of Sverdrup & Parcel and Associates, Inc.), contract operator of the Arnold Engineering Development Center (AEDC), Air Force Systems Command (AFSC), Arnold Air Force Station, Tennessee, under Contract F40600-71-C-0002. The experimental work was conducted from October 7 to 15, 1970, and the coordination of the data reduction with AFCRL was completed on December 15, 1970. The work was conducted under ARO Project No. VP0150, and the manuscript was submitted for publication on February 19, 1971.

T. P. Condron, coauthor of this report, is an employee of the United States Air Force at AFCRL.

This technical report has been reviewed and is approved.

Emmett A. Niblack, Jr.  
Lt Colonel, USAF  
AF Representative, VKF  
Directorate of Test

Joseph R. Henry  
Colonel, USAF  
Director of Test

## ABSTRACT

The final preflight calibration tests of the ARPA/AFCRL CVF II spectroradiometer were performed in the Aerospace Research Chamber (7V). These tests included linearity, absolute responsivity, angular response, frequency response, and wavelength calibration. The measured field of view was 8.4 deg or  $1.69 \times 10^{-2}$  sr with an off-axis rejection ratio of  $10^{-5}$  at 34 deg off axis. The instrument was linear over most of its range, but displayed nonlinearity for high irradiance levels. Wavelength calibration was found to have not changed significantly from a previous calibration. The absolute responsivity at  $6.10 \mu\text{m}$  was found to be  $4.7 \times 10^{11} \text{ v/w/cm}^2\text{-}\mu\text{m}$ , and spectral responsivity was calculated based on this value in combination with relative spectral data obtained during a previous test.

This document may be further distributed by any holder  
only with specific prior approval of Air Force  
Cambridge Research Laboratories (CRRL), L. G.  
Hanscom Field, Bedford, Massachusetts 01730.

## CONTENTS

	<u>Page</u>
ABSTRACT . . . . .	iii
NOMENCLATURE . . . . .	vi
I. INTRODUCTION . . . . .	1
II. APPARATUS . . . . .	1
III. PROCEDURE . . . . .	4
IV. RESULTS AND DISCUSSION . . . . .	5
V. SUMMARY . . . . .	9
REFERENCES . . . . .	9

## APPENDIXES

## I. ILLUSTRATIONS

Figure

1. Aerospace Research Chamber (7V) . . . . .	13
2. Detector Output versus Spectral Irradiance, $\lambda = 8.49 \mu\text{m}$ , First Pumpdown . . . . .	14
3. Detector Output versus Spectral Irradiance, $\lambda = 6.10 \mu\text{m}$ , Second Pumpdown . . . . .	15
4. Normalized Transfer Function, HS-1 Spectroradiometer . . . . .	16
5. Polar Angle versus Mirror Position, 7V Chamber . . . . .	17
6. HS-1 Angular Response, Target Source . . . . .	18
7. HS-1 Angular Response, Solar Source . . . . .	19
8. HS-1 Angular Response . . . . .	20
9. HS-1 Spectral Irradiance Responsivity . . . . .	21
10. HS-1 Inverse Spectral Radiance Responsivity . . . . .	22
11. Frequency Response of HS-1 Spectroradiometer . . . . .	23
12. Wavelength Calibration. . . . .	24

Page

## II. TABLES

I. HS-1 Angular Response . . . . .	25
II. HS-1 Off-Axis Rejection. . . . .	26
III. Wavelength Calibration Data. . . . .	27

## NOMENCLATURE

A	Attenuation factor
$C_\lambda$	Inverse spectral radiance responsivity, $w/cm^2\text{-}\mu m\text{-sr}\text{-v}$
$E_\lambda$	Target spectral irradiance at sensor aperture, $w/cm^2\text{-}\mu m$
$L_\lambda$	Spectral radiance, $w/cm^2\text{-}\mu m\text{-sr}$
$V_T$	Signal voltage attributable to target irradiance
$f(V)$	Voltage linearizing function
$\theta$	Off-axis angle of incoming radiation

## SECTION I INTRODUCTION

The Air Force Cambridge Research Laboratory and ARPA are engaged in the development of an infrared spectrometer for studies of the infrared emittance and reflectance of the earth's upper atmosphere. The sensor development work is being carried out by Utah State University and features a liquid-helium-cooled, mercury doped germanium detector and a rotating circular variable filter (CVF) for spectral scans in the 4- to 13-micron range. The filter is an interference type with a film of continuously variable thickness. An optical pulse generator is used to correlate filter position with detector output, and the detector output is channeled through series amplifiers providing four output channels with gains of 1, 10, 100, and 1000 (referred to as Gains 1, 2, 3, and 4, respectively).

Testing of the first-generation CVF spectrometer, Utah State Model WW-12, was accomplished at AFCRL and also at AEDC (Refs. 1 and 2). The current test is the final preflight test of the second-generation spectrometer, the Utah State Model HS-1, which incorporated mechanical and electronic improvements over the WW-12. Two previous tests of the HS-1 have been accomplished at AEDC. The first test (Ref. 3) showed unacceptable noise levels on the two highest gain channels. Modifications were made and the sensor was returned for the second test (Ref. 4). As a result of these tests, it was decided that further modifications were required, necessitating the current test. These modifications included removal of optical baffle tubes and other changes to the optical system to increase responsivity by widening the field of view.

Objectives of the current test were to determine linearity, absolute responsivity, angular response, spectral response, frequency response, and filter wheel wavelength calibration. Wavelength calibration required use of a series of narrow bandpass filters furnished by AFCRL to correlate the optical pulse generator with the CVF position.

## SECTION II APPARATUS

### 2.1 AEROSPACE RESEARCH CHAMBER (7V)

The Aerospace Research Chamber (7V) (Fig. 1, Appendix I) consists of four integrated systems which are used for testing long wavelength infrared (LWIR) sensors.

### **2.1.1 Chamber**

Chamber 7V is a stainless steel horizontal chamber 7 ft in diameter by 12 ft in length with access provided by a 7-ft-diam door on each end of the chamber. A 2-ft-diam by 6-ft-long cylinder has been installed in the east door. Equipped with an isolation valve, this ante-chamber permits the return of a test article (sensor) to ambient conditions while the main chamber and the LWIR simulator equipment remain at test pressure and temperature.

A liquid-nitrogen-cooled shroud, approximately 74 in. in diameter and 12 ft long, lines the chamber and operates at approximately 77°K. Inside the liquid-nitrogen-cooled shroud is a gaseous-helium-cooled liner which is maintained at 20°K. The helium-cooled liner is fabricated from extruded aluminum finned tube material and is 10 ft long with an inner diameter of approximately 66 in.

### **2.1.2 Pumping System**

Evacuation of the chamber is accomplished by two 260-liter/sec turbomolecular pumps backed by a lobe-type blower which, in turn, is backed by a 140-cfm mechanical vacuum pump. This "dry" pumping system prevents sensor optical system contamination. Additional pumping in the form of cryopumping is provided by the liquid-nitrogen-cooled and gaseous-helium-cooled liners. The large cryopumping capacity provides the low pressures ( $10^{-8}$  torr) at which most of the tests are performed.

### **2.1.3 Refrigeration System**

The liquid nitrogen is supplied from a 13,000-gal storage tank; the boil-off gas is reliquefied and returned to the tank. The gaseous helium may be supplied from one of two 4-kw refrigeration units or from a 1-kw unit. The liquid helium required for sensors under test is provided by an in-house helium liquefier unit.

### **2.1.4 LWIR Target Simulator System**

This system consists of a target or source simulator and a solar and earth radiation simulator. The target or source simulator has the following performance specifications:

Resolution	0.5 milliradians
Field of View	5 deg by 5 deg
Rate of Motion	0 to 1 deg/sec
Modulation Frequency	10 to 500 Hz
Target Temperature Range	Classified
Irradiance Range	Classified

Background and stray radiation is controlled with helium-cooled baffles as required.

The solar and earth radiation simulator has the following performance specifications:

Beam Diameter	10 $\pm$ 1/2 in.
Angular Displacement (Beam)	0 to 70 deg (in horizontal plane)
Decollimation Angle	$\pm$ 3 deg max
Uniformity	$\pm$ 10 percent
Irradiance (at sensor)	
Solar	Total: 0.14 w/cm <sup>2</sup> 8 to 14 $\mu$ m: $1.15 \times 10^{-4}$ w/cm <sup>2</sup>
Earth	Total: $5.6 \times 10^{-4}$ w/cm <sup>2</sup> 8 to 14 $\mu$ m: $2 \times 10^{-5}$ w/cm <sup>2</sup>

## 2.2 SENSOR INSTALLATION

The sensor was installed in the Chamber 7V antechamber with its cooled front face inserted through an optically tight mating baffle on the chamber liner end plate. The instrument was thermally and electrically insulated from the liner baffle and the antechamber instrument support structure. The sensor liquid helium supply and vent lines were electrically isolated inside the antechamber by using specially fabricated couplings developed for this test. This eliminated the unshielded external liquid helium dewar as the probable antenna for the 60-Hz noise observed on the previous test. Except for the liquid helium system, the sensor mounting hardware with remote vertical adjustment from the previous HS-1 test (Ref. 4) was used.

## 2.3 INSTRUMENTATION

All sensor outputs were routed to the Chamber 7V data room. The four detector output channels were selectively patched into one channel on an oscilloscope, with the filter position reference and calibration reset reference displayed on two other channels. A two-channel memory oscilloscope was used to monitor detector output during adjustment of

chamber parameters, then one or more filter wheel scans of the sensor were recorded on the oscillograph. Chamber data (target temperature, target coordinates, and solar boom position) and the sensor temperature data (detector temperature, baffle temperature, and filter drive motor temperature) were printed out on a multichannel scanning recorder. The scanning was manually initiated once for each recorded oscillograph run, with sequence number and time recorded on both for correlation.

### SECTION III PROCEDURE

Two pumpdowns were required to complete the test. During the first pumpdown, a low level 300°K spectrum was obtained with the instrument looking at chamber background, and it was concluded that the baffling between chamber and sensor was inadequate. Since the leak did not saturate the instrument except on gain 4, and further, did not cover the entire instrument spectrum, it was decided to get as much data as possible. The target source chopper was used to discriminate between target and background.

On attempting to measure the field of view, however, it was found that the field of view was larger than the predicted 4 deg and could not be measured with the target movement system which scans 5 deg. In addition, the responsivity was much lower than predicted. Data on linearity and spectral response were taken, but it was decided to disassemble the sensor and retest during a second pumpdown. During the downtime, the sensor baffles were lined to reduce radiation leaks, and the chamber collimating mirror movement system was activated to allow measurement of a large field of view.

Sensor disassembly and checkout revealed a detector bias resistor which should have been  $10^9$  ohms was  $10^8$  ohms, and this was replaced with one of the proper value. In addition, the filter drive motor was found to have overheated and leaked oil from its gearbox into the sensor. This is believed to have resulted from nearly continuous operation with the sensor case maintained slightly above room temperature. The motor was replaced and a temperature monitor installed on the motor case.

On achieving test conditions on the second pumpdown, it was found that the 300°K radiation leak had not been corrected, and greater sensor responsivity had increased its effect. However, it was decided to work around the affected portions of the spectrum as before and proceed with the test. Subsequent investigation disclosed a missing bolt in the 20°K chamber baffle mount had allowed the 300°K radiation leak.

Data for linearity, angular response, and frequency were taken at one wavelength selected such that response was unaffected by the radiation leak. These parameters are unlikely to be a function of wavelength. Wavelength calibration of the chopper was unaffected by the leak since it is only necessary to correlate the chopper pulses with the signal spikes resulting from use of the narrow bandpass calibration filters, and signal level is unimportant.

The radiation leak did preclude obtaining a reliable absolute spectral response calibration. Since a calibration had previously been obtained (Ref. 3) and since the optical materials and detector elements were unchanged, it was decided to reproduce the previously obtained response curve and ratio each point according to the response ratio at the wavelength used for the current linearity test. Some spectral response data were obtained during the first pumpdown, and these were used to verify the curve shape.

## SECTION IV RESULTS AND DISCUSSION

### 4.1 RESPONSE LINEARITY AND ABSOLUTE RESPONSIVITY

During the first pumpdown, the wavelength used for checking linearity was  $8.49 \mu\text{m}$  - where the effect of the  $300^\circ\text{K}$  leak could be avoided reasonably well. A plot of target spectral irradiance,  $E_\lambda$ , versus the voltage attributable to the target,  $V_T$ , is shown in Fig. 2.

In addition to the data points obtained, an array of four 45-deg-slope straight lines is shown separated by factors of 10, the gain factors for the HS-1. Any slope other than 45 deg on the plot would indicate a nonlinear relationship between  $E_\lambda$  and  $V_T$ . The HS-1 appears to have a linear response on Gain 3 and probably on Gain 4; the point at 0.66 v on that gain should not be given much weight because the target signal to radiation leak ratio is only unity for that point. Gain 2 is probably linear up to a voltage of 0.5 v and then shows a nonlinear trend. The two points on Gain 1 also indicate nonlinearity. The inverse spectral irradiance responsivity on the highest gain during this test was  $1.55 \times 10^{-11} \text{ w-cm}^{-2} \mu\text{m}^{-1}\text{-v}^{-1}$  at a wavelength of  $8.49 \mu\text{m}$ .

For the second pumpdown the radiation leak did not permit use of the  $8.49\text{-}\mu\text{m}$  wavelength; the increase in gain attributable to the installation of the  $10^9$  ohm bias resistor resulted in a background signal which was too high. Therefore, a shorter wavelength,  $6.1 \mu\text{m}$ , was used. The

results of this test are shown in Fig. 3. Gains 2 and 3 both appear to be linear all the way in the increased sensitivity configuration, but Gain 1 exhibits considerable nonlinearity above 1 v. During this test the background leak at  $6.1 \mu\text{m}$  caused a 1.13-v output on Gain 4 and the HS-1 went into hard saturation over practically all of its spectral range. This resulted in very erratic readings at  $6.1 \mu\text{m}$  during the short period of time when it was out of saturation; hence, no valid points were obtained for Gain 4. However, it is reasonable to assume that the gain factor of 10 which applied during the first pumpdown would still apply during the second pumpdown. A line has therefore been drawn for that gain.

The inverse spectral irradiance responsivity at  $6.1 \mu\text{m}$  was  $2.15 \times 10^{-12} \text{ w-cm}^{-2}\text{-}\mu\text{m}^{-1}\text{-v}^{-1}$  on Gain 4 for the second pumpdown. Since the response, based on the April 1970 calibration (Ref. 3), is 1.9 times as great at  $8.49 \mu\text{m}$  as it is at  $6.1 \mu\text{m}$ , the inverse response at  $8.49 \mu\text{m}$  would be  $1.13 \times 10^{-12} \text{ w-cm}^{-2}\text{-}\mu\text{m}^{-1}\text{-v}^{-1}$ . Therefore, an increase in sensitivity of a factor of 14 was obtained by installing the new bias resistor.

Once the nonlinearity of Gain 1 was discovered, it would have been desirable to avoid that gain for all subsequent calibration procedures. This was impossible to do in the field-of-view measurement procedures without throwing away useful data. Therefore, a convenient way to remove the nonlinearity from the data taken on Gain 1 was devised. The method found most convenient for this purpose was to introduce a quantity  $f(V)$  which is linearly related to the power incident on the detector. This was accomplished by shifting the four curves of Fig. 3 to the left such that the Gain 4 curve intersects  $E_\lambda = 10^{-12}$  at an ordinate value of 1 v. The results are shown in Fig. 4 where the entire plot has been normalized to the Gain 4 line at 1 v. The points have been left off Fig. 4 for Gains 2, 3, and 4 because they are of no further use once it is defined that  $E_\lambda = 2.15 \times 10^{-12} \text{ w-cm}^{-2}\text{-}\mu\text{m}^{-1}$  for  $f(V) = 1$ ;  $E_\lambda$  for any other voltage and gain is simply  $2.15 \times 10^{-12} f(V)$ . However, the points of Gain 1 are needed to determine  $f(V)$  for that gain. The point on Gain 1 at  $f(V) = 1.6 \times 10^2$  does not quite fall into place, but it is a small voltage and it is known from the Gain 2 points in that region that the instrument is linearly responsive for  $f(V) = 5 \times 10^2$ . The result is a set of curves allowing conversion of  $V_T$  to a quantity  $f(V)$  which is simply a constant times the power incident on the detector and is therefore linearly related to that power.

The next step in the process is to eliminate the need for reading the  $f(V)$  plot in the range where  $V_T$  is already linearly related to the

input power, viz., Gains 2, 3, and 4, and for voltages less than or equal to 0.78 v on Gain 1. This can be accomplished by introducing attenuation factors A as follows:

<u>Gain</u>	<u>A</u>
1	$7.3 \times 10^2$
2	$10^2$
3	10
4	1.0

The irradiance at  $6.1 \mu\text{m}$  is then

$$E_\lambda = 2.15 \times 10^{-12} (\text{AV}_T) \text{ for } \text{AV}_T 7.3 \times 10^2 \times 0.78 = 5.7 \times 10^2$$

which is the f(V) value (Fig. 4) above which the HS-1 becomes nonlinear. In reducing calibration data or flight data, therefore, all that is necessary is to take the product of the target voltage and the appropriate value of A and then multiply the product by the constant which applies for the wavelength in question (for Gains 2, 3, and 4 and for  $V_T = 0.78$  v on Gain 1). For voltages greater than 0.78 v on Gain 1 the formula which applies at  $6.1 \mu\text{m}$  is

$$E_\lambda = 2.15 \times 10^{-12} f(V)$$

which is the general formula applying to the entire dynamic range of the radiometer since  $f(V) = V_T A$  for the entire linear range. In all subsequent calibration procedures  $V_T$  is reduced to f(V) before the data are processed.

#### 4.2 THE HS-1 ANGULAR RESPONSE

A tabulation of the angular response data obtained by rotating the large chamber collimating mirror is given in Table I, Appendix II, where the conversion from the distance through which the mirror moved to angle was computed using Fig. 5. The normalized angular response is plotted versus the off-axis angle,  $\theta$ , in Fig. 6 where the effective solid angle,  $\Omega_{\text{eff}}$ , is  $1.69 \times 10^{-2}$  sr. The data obtained with the solar source are tabulated in Table II and plotted in Fig. 7. A composite plot based on both sources is given in Fig. 8 and shows an off-axis rejection ratio of  $10^{-5}$  by 34 deg off axis.

#### 4.3 ABSOLUTE SPECTRAL RESPONSE

The HS-1 absolute spectral irradiance responsivity is plotted versus wavelength in Fig. 9. The shape of the curve was copied from the

original HS-1 absolute response determination of April 1970 (Ref. 3), and the points are those obtained using a 606°K source during the first pumpdown. The absolute value for the curve is based on the multitude of points obtained at  $6.1 \mu\text{m}$  during the second pumpdown (after the new bias resistor had been installed); that value was  $2.15 \times 10^{-12} \text{ w-cm}^{-2} \mu\text{m}^{-1} \text{-v}^{-1}$ , resulting in  $1/(2.15 \times 10^{-12}) = 4.65 \times 10^{11} \text{ v/w-cm}^{-2} \mu\text{m}^{-1}$  at  $6.1 \mu\text{m}$ . The inverse spectral radiance responsivity is plotted versus wavelength in Fig. 10. The value at  $6.1 \mu\text{m}$  is determined by dividing  $2.15 \times 10^{-12}$  by the HS-1 effective solid angle, i. e.,  $2.15 \times 10^{-12} / 1.69 \times 10^{-2} = 1.27 \times 10^{-10} \text{ w-cm}^{-1} \text{-sr}^{-1} \mu\text{m}^{-1} / \text{v}$  on Gain 4. The ordinate is labelled  $C_\lambda$  for use in the equation

$$L_\lambda = C_\lambda f(V) \quad \text{w-cm}^{-2} \text{-sr}^{-1} \mu\text{m}^{-1}$$

#### 4.4 RADIOMETER FREQUENCY RESPONSE

The normalized response of the HS-1 spectroradiometer as a function of frequency is given in Fig. 11. The data were obtained by chopping the source at the frequencies indicated by the points. The response was 3 db down at 100 Hz, and the roll-off at the higher frequencies is approximately 10 db/octave.

#### 4.5 WAVELENGTH CALIBRATION

The wavelength calibration was obtained by using a series of six narrow bandpass filters in front of the target. The location of the resulting signal spike during a spectrometer scan is then correlated to the chopped reference signal. This signal is obtained from a chopper rigidly connected to the filter wheel, with the chopper containing one wide blade for reference. From previous tests the rise to the short-voltage pulse has been defined as No. 7, since this places No. 1 pulse at the lowest wavelength to start the spectral scan. Results of the current calibration are shown in Fig. 12, with the previous calibration (Ref. 3) also shown.

It appears that a slight rotational shift has occurred. The data are also presented in Table III where the apparent errors have been tabulated. AFCRL is currently checking the wavelength calibration of the narrow bandpass filters.

Investigation of the raw data revealed a change in the ratio of the on-off time for the chopper pulses. The chopper has ten blades including one wide blade. During previous tests (Refs. 3 and 4) the ratio

of photocell on to off time was 1.86 for nine blades and 0.68 for the wide blade. During the current test, however, the ratio was 1.173 for nine blades and 0.51 for the wide blade.

## SECTION V SUMMARY

These tests comprise the final preflight calibration of the HS-1 spectroradiometer. The calibration data obtained on spectral response, linearity, and wavelength calibration are required for meaningful reduction of data from orbit. Of particular significance are the larger-than-expected field of view and the detection and replacement of the incorrect feedback resistor.

## REFERENCES

1. Condon, T. P. "Post Flight Calibration of the AFCRL CVF Radiometer." Air Force Cambridge Research Laboratories Report, February 1970.
2. Warner, R. M. "Calibration of AFCRL First-Generation Circular Variable Filter Spectrometer." AEDC-TR-70-152, August 1970.
3. Warner, R. M. "Calibration of ARPA/AFCRL Second-Generation Circular Variable Filter Spectrometer." AEDC-TR-70-200, September 1970.
4. Arnold, F. "Baffling Test and Calibration of ARPA/AFCRL CVF II Spectrometer." AEDC-TR-71-1, February 1971.

**APPENDIXES**  
**I. ILLUSTRATIONS**  
**II. TABLES**

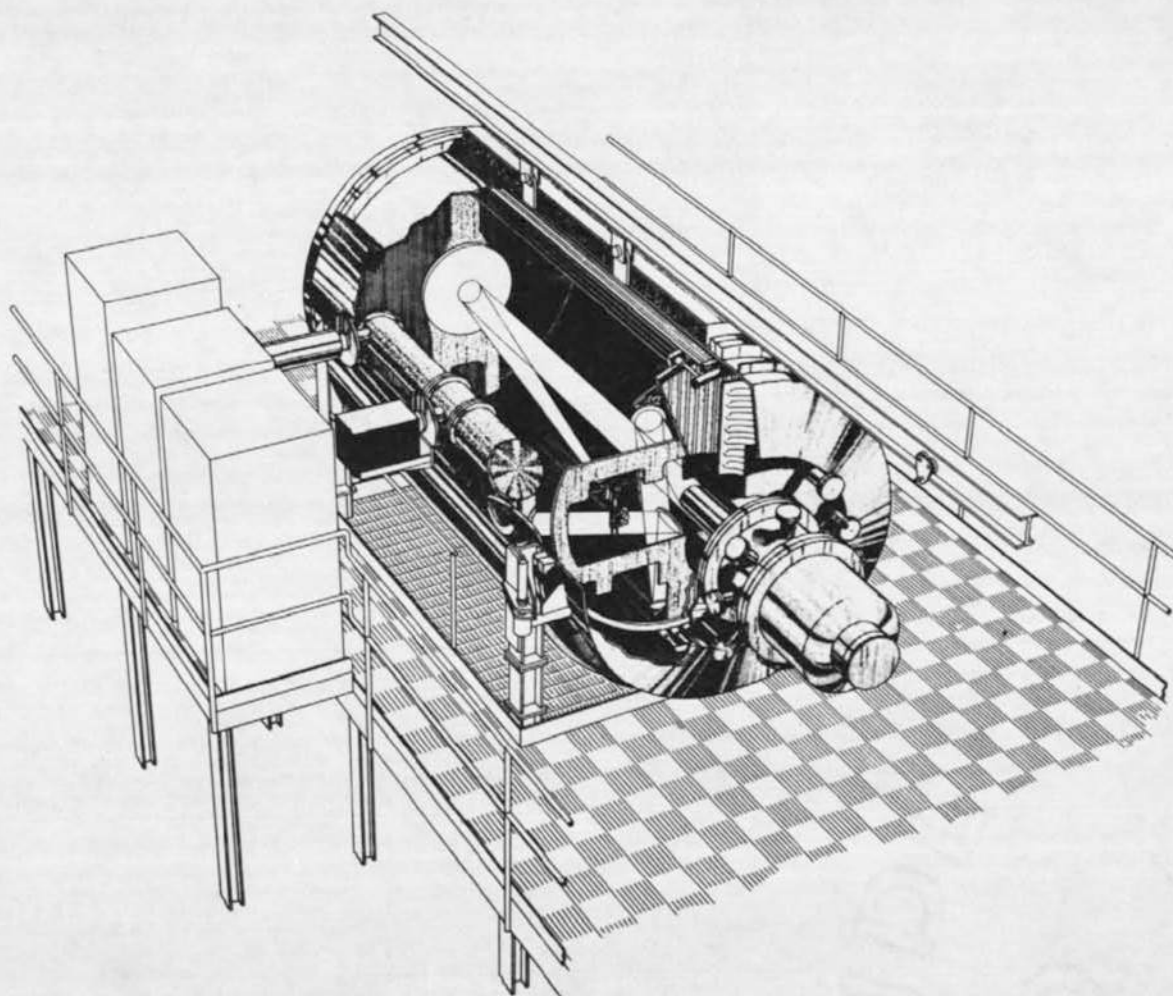


Fig. 1 Aerospace Research Chamber (7V)

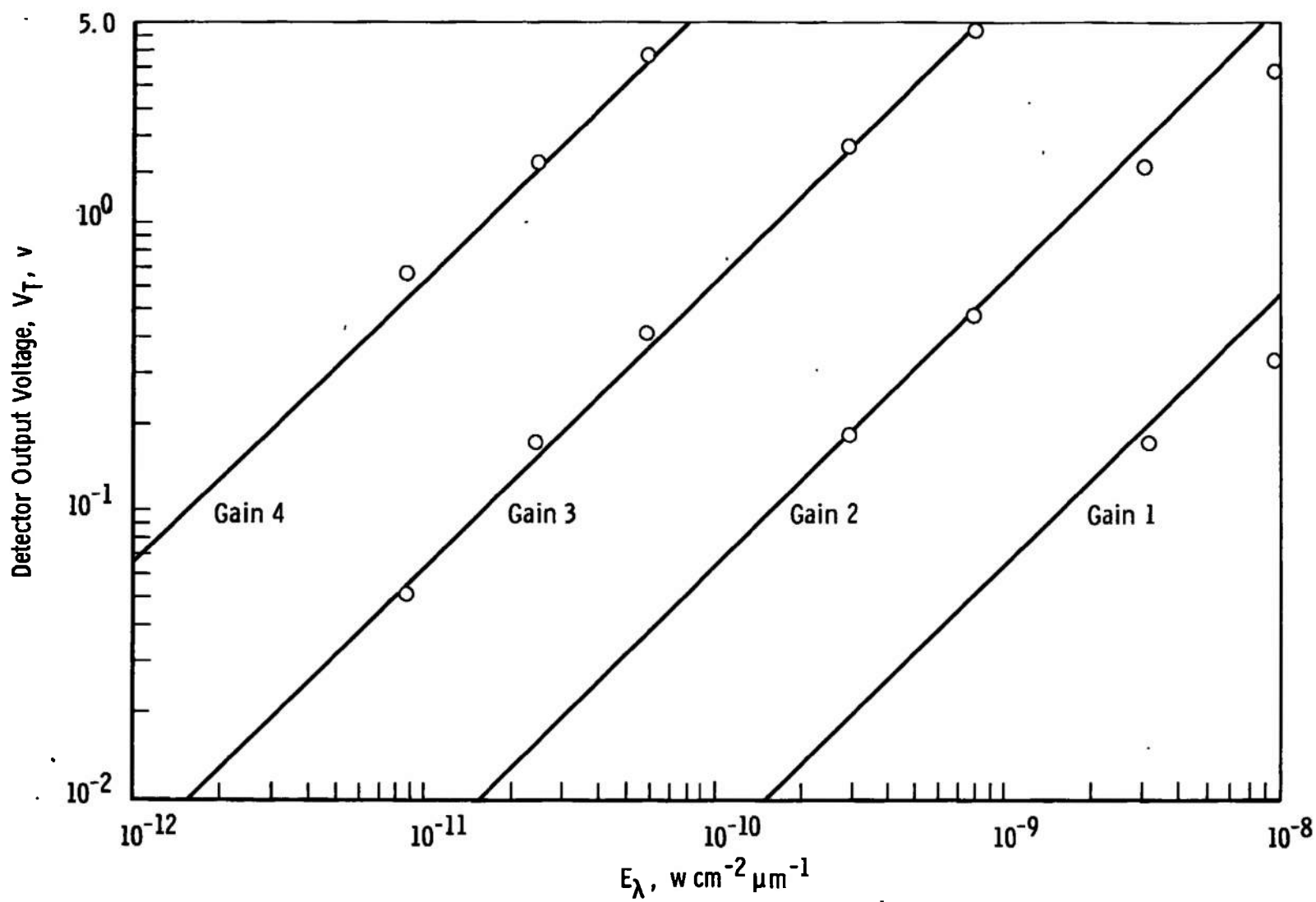


Fig. 2 Detector Output versus Spectral Irradiance,  $\lambda = 8.49 \mu\text{m}$ , First Pumpdown

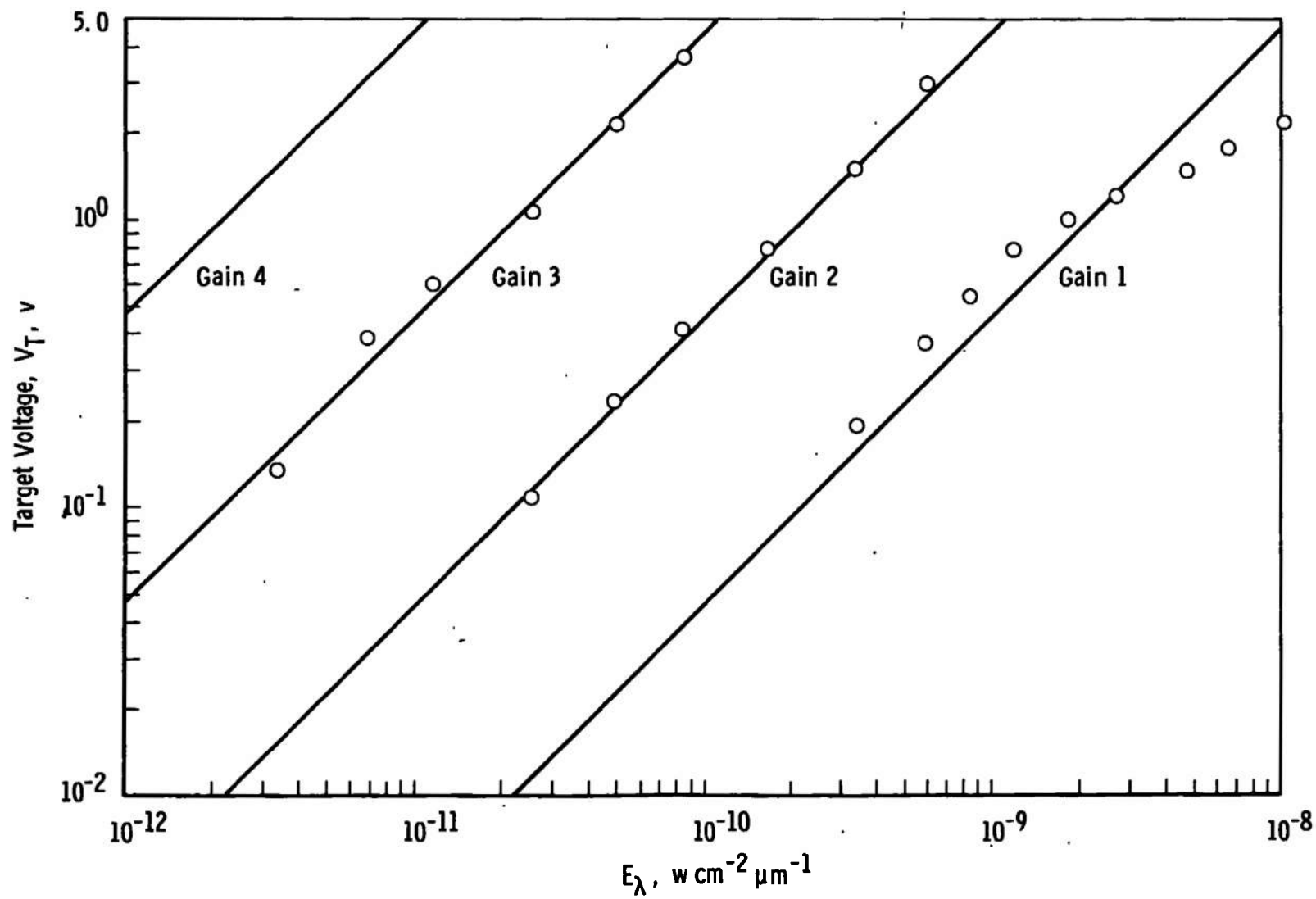


Fig. 3 Detector Output versus Spectral Irradiance,  $\lambda = 6.10 \mu\text{m}$ , Second Pumpdown

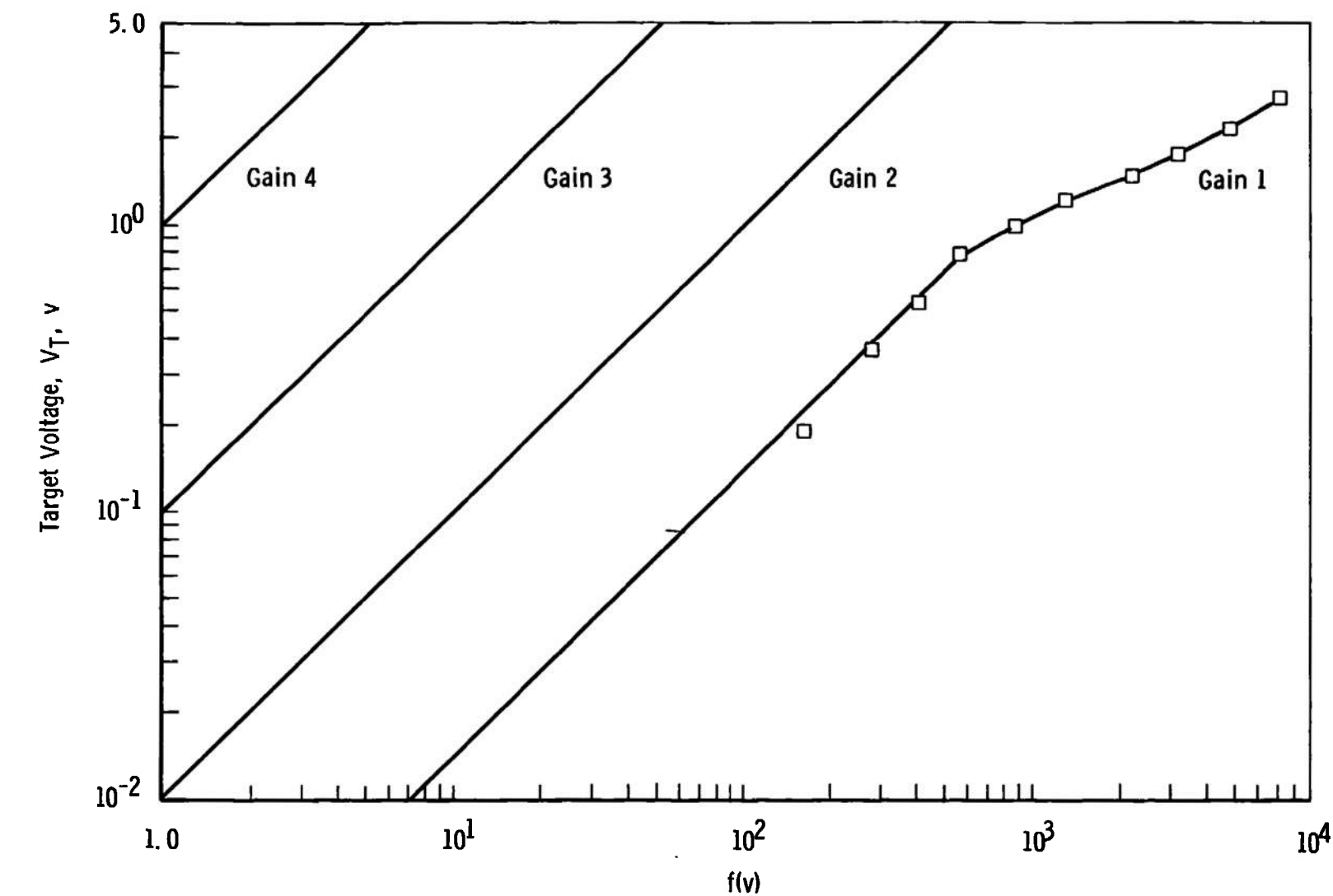


Fig. 4 Normalized Transfer Function, HS-1 Spectroradiometer

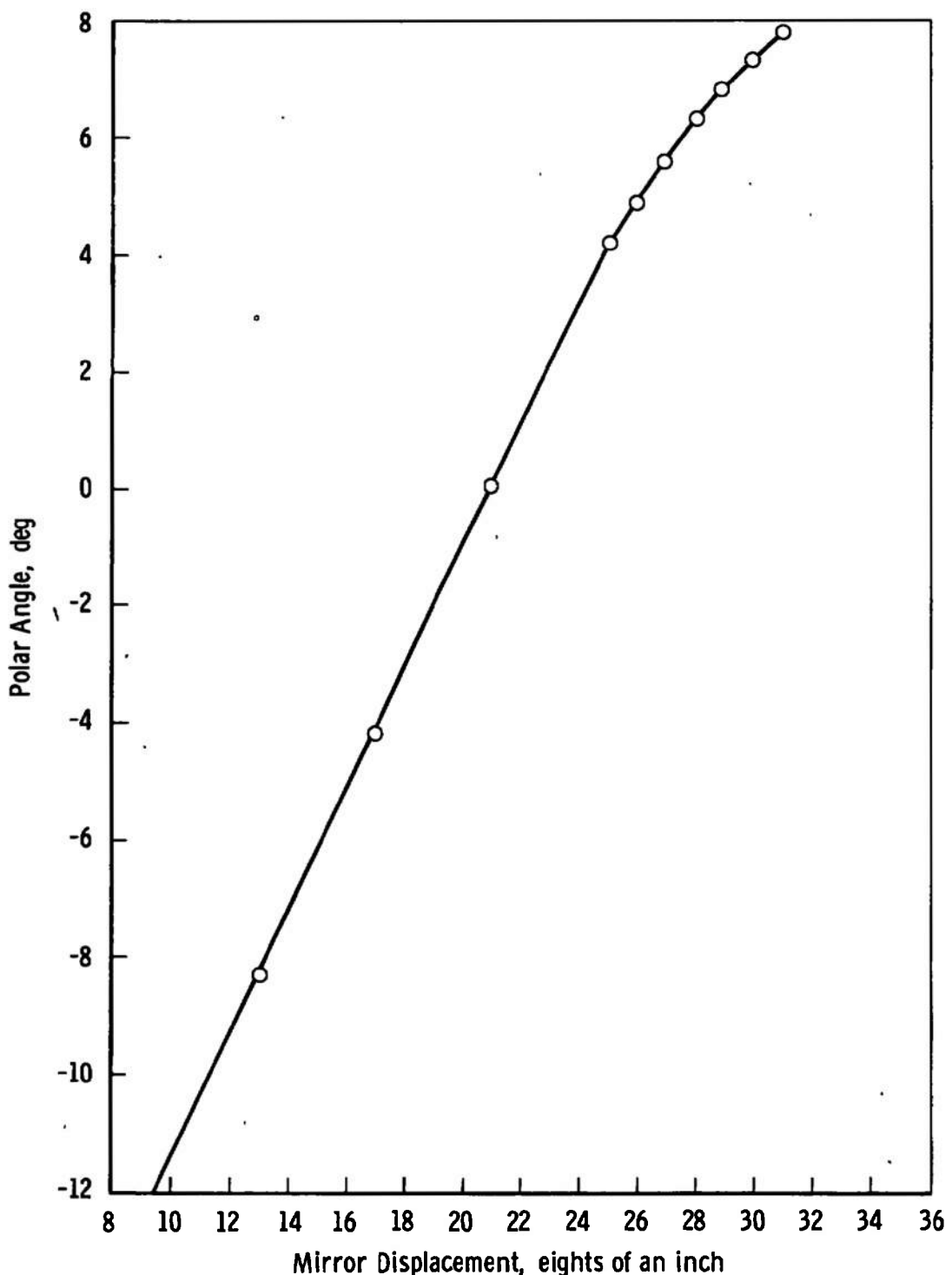


Fig. 5 Polar Angle versus Mirror Position, 7V Chamber

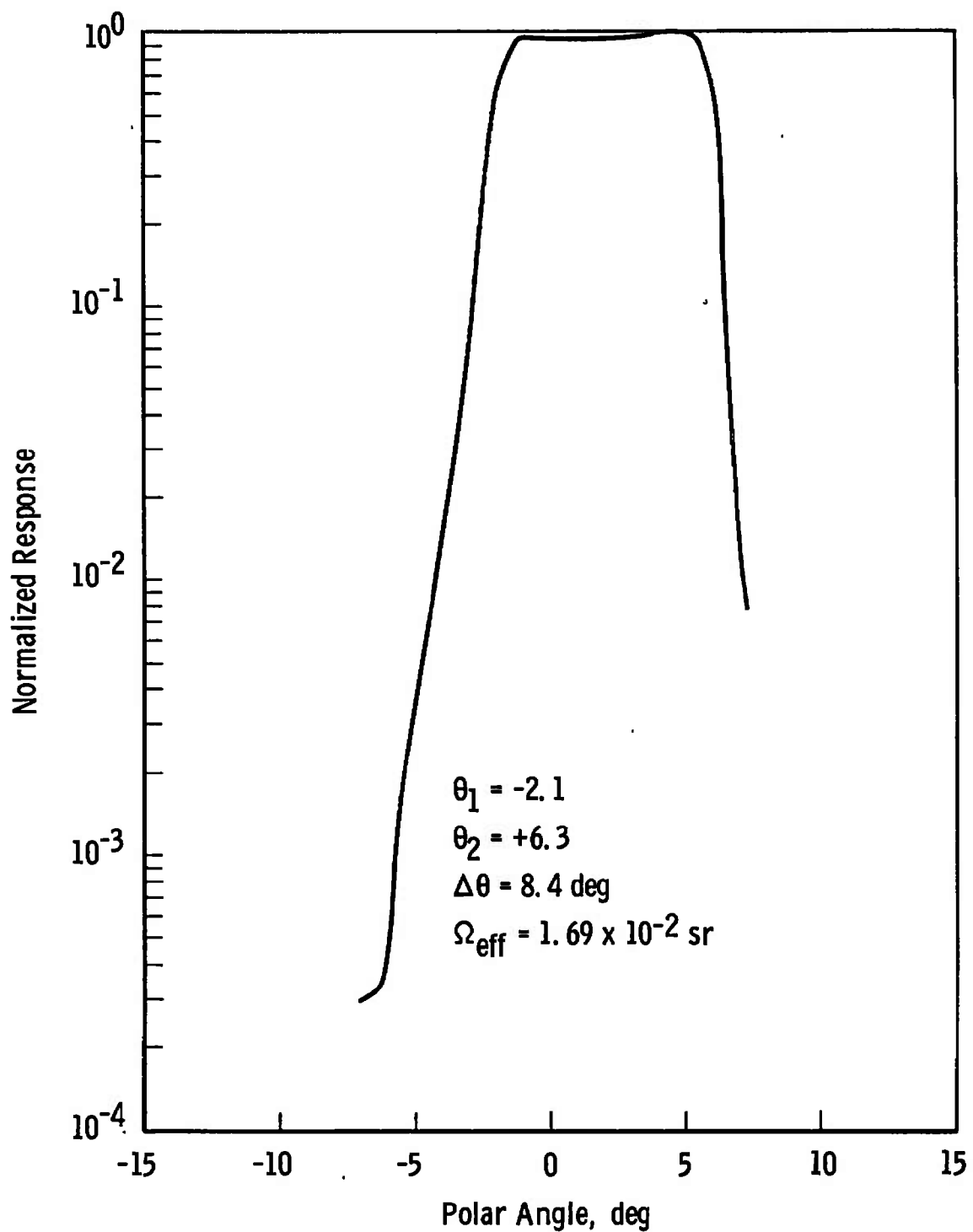


Fig. 6 HS-1 Angular Response, Target Source

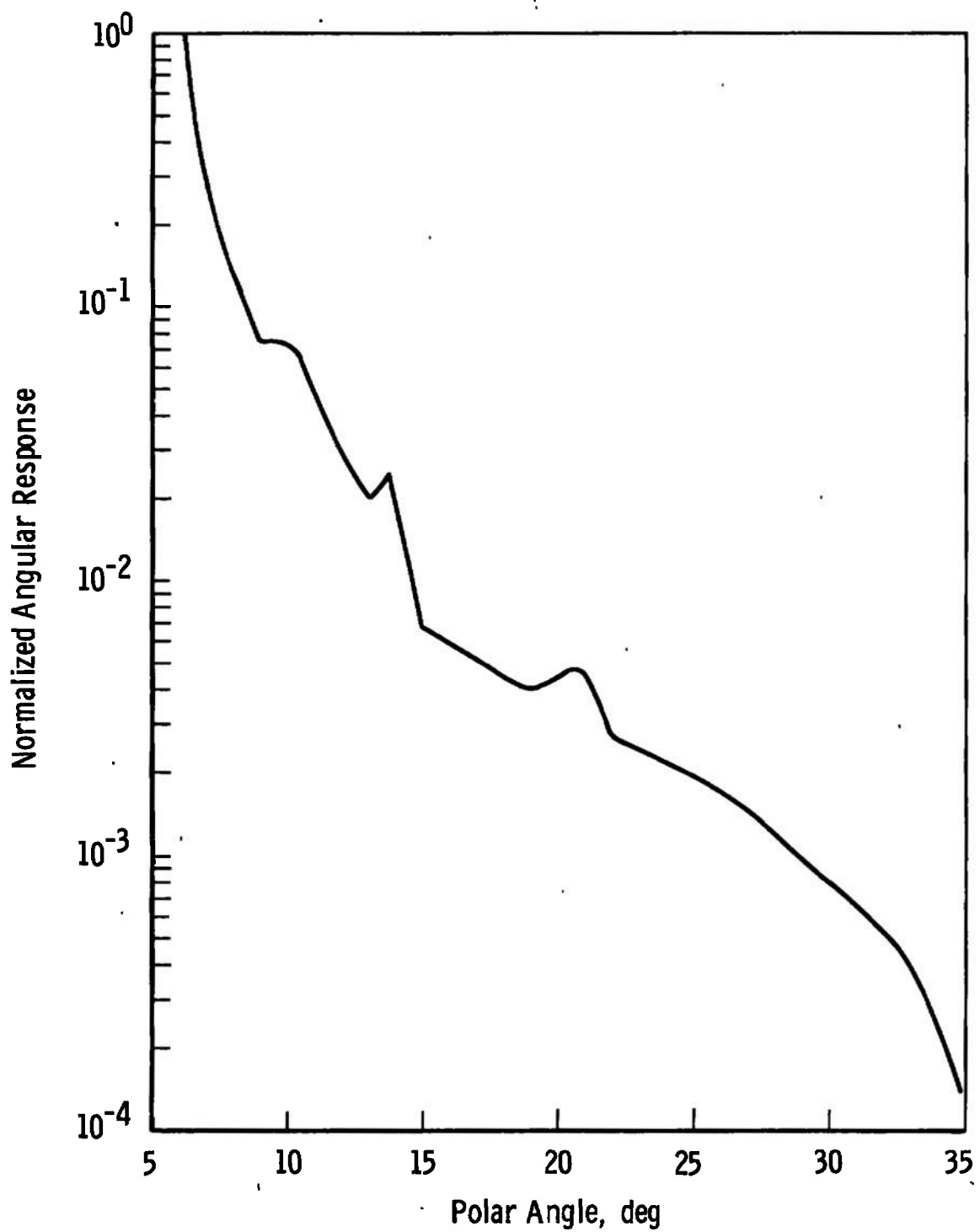
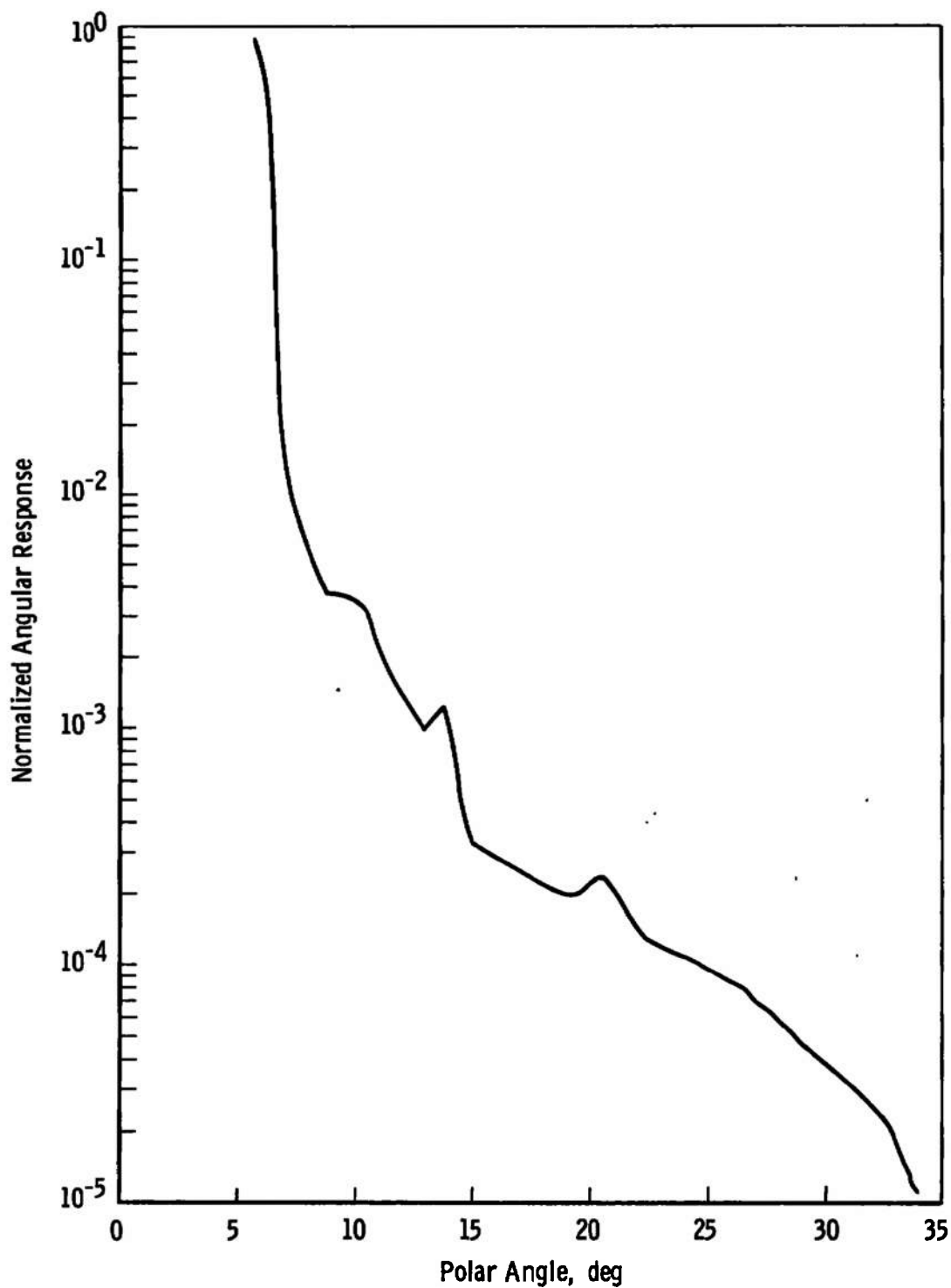


Fig. 7 HS-1 Angular Response, Solar Source



**Fig. 8 HS-1 Angular Response**

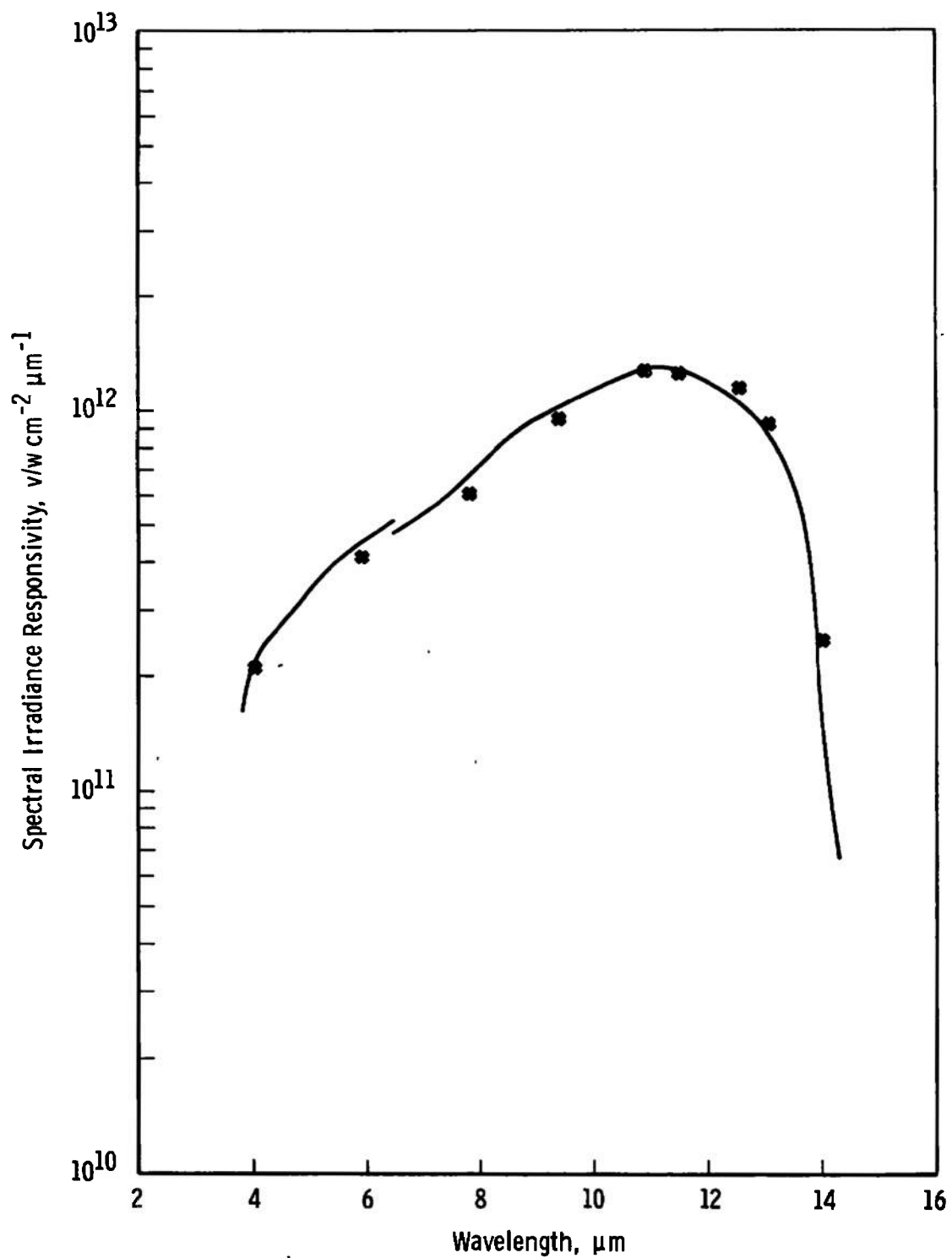


Fig. 9 HS-1 Spectral Irradiance Responsivity

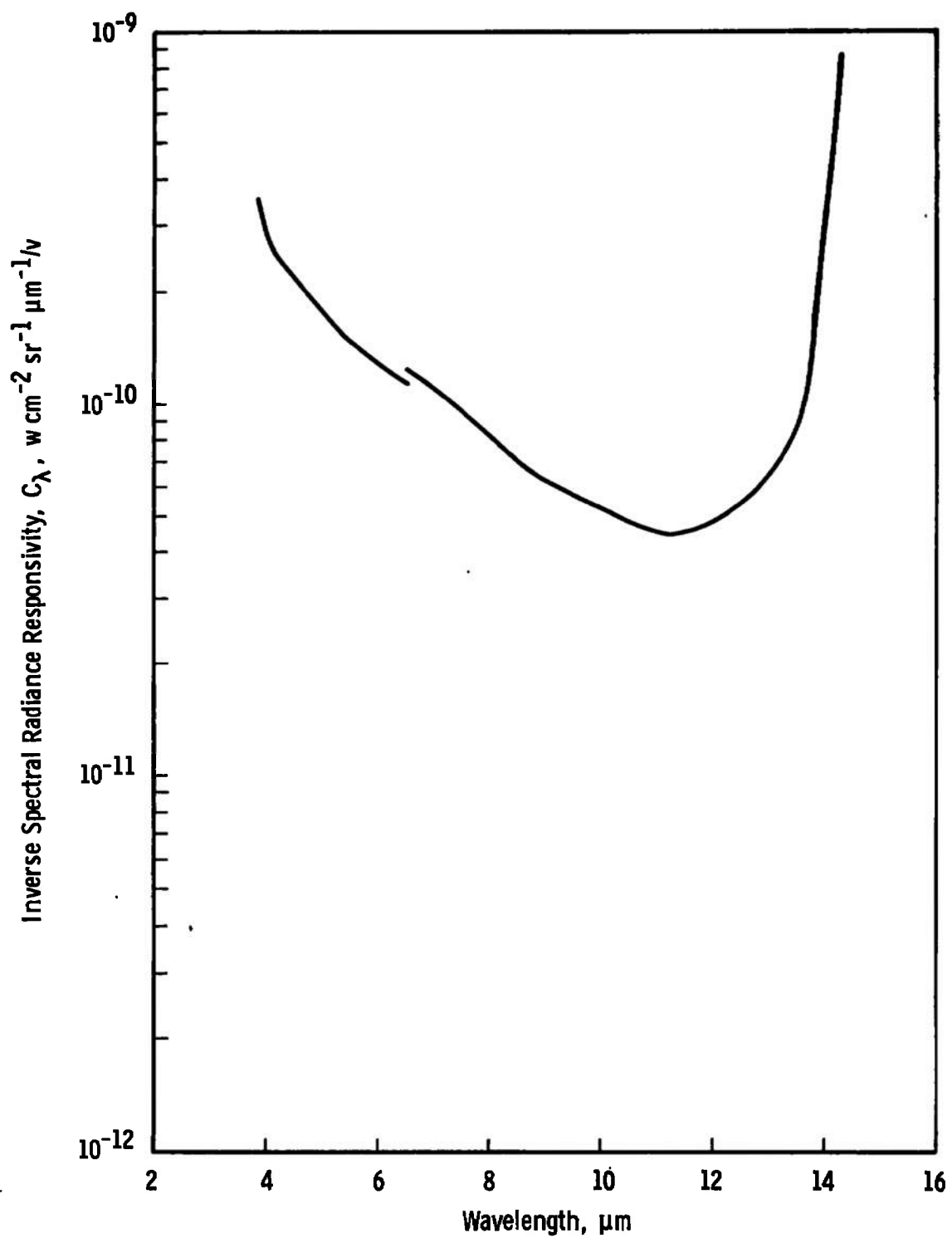


Fig. 10 HS-1 Inverse Spectral Radiance Responsivity

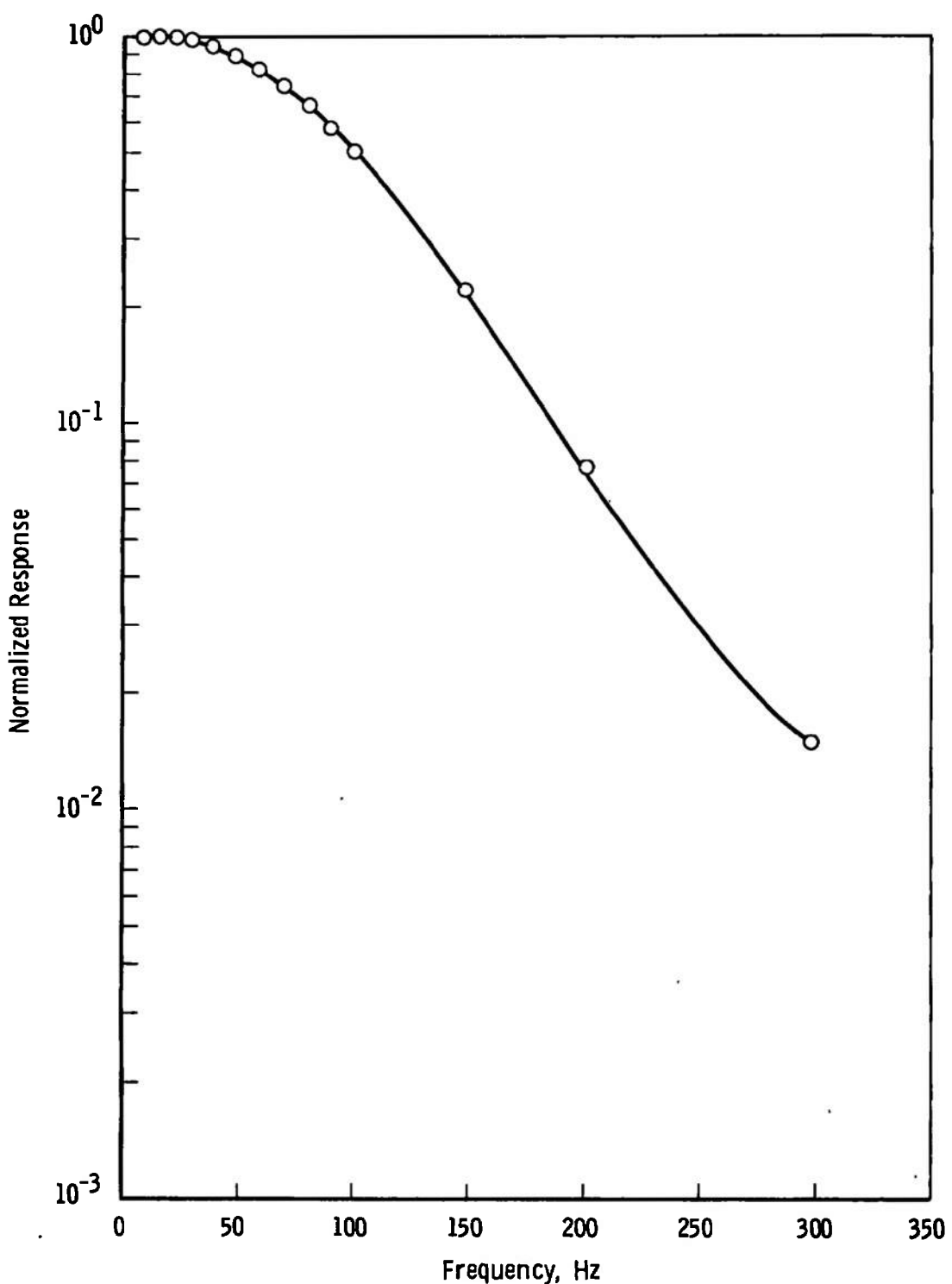


Fig. 11 Frequency Response of HS-1 Spectroradiometer

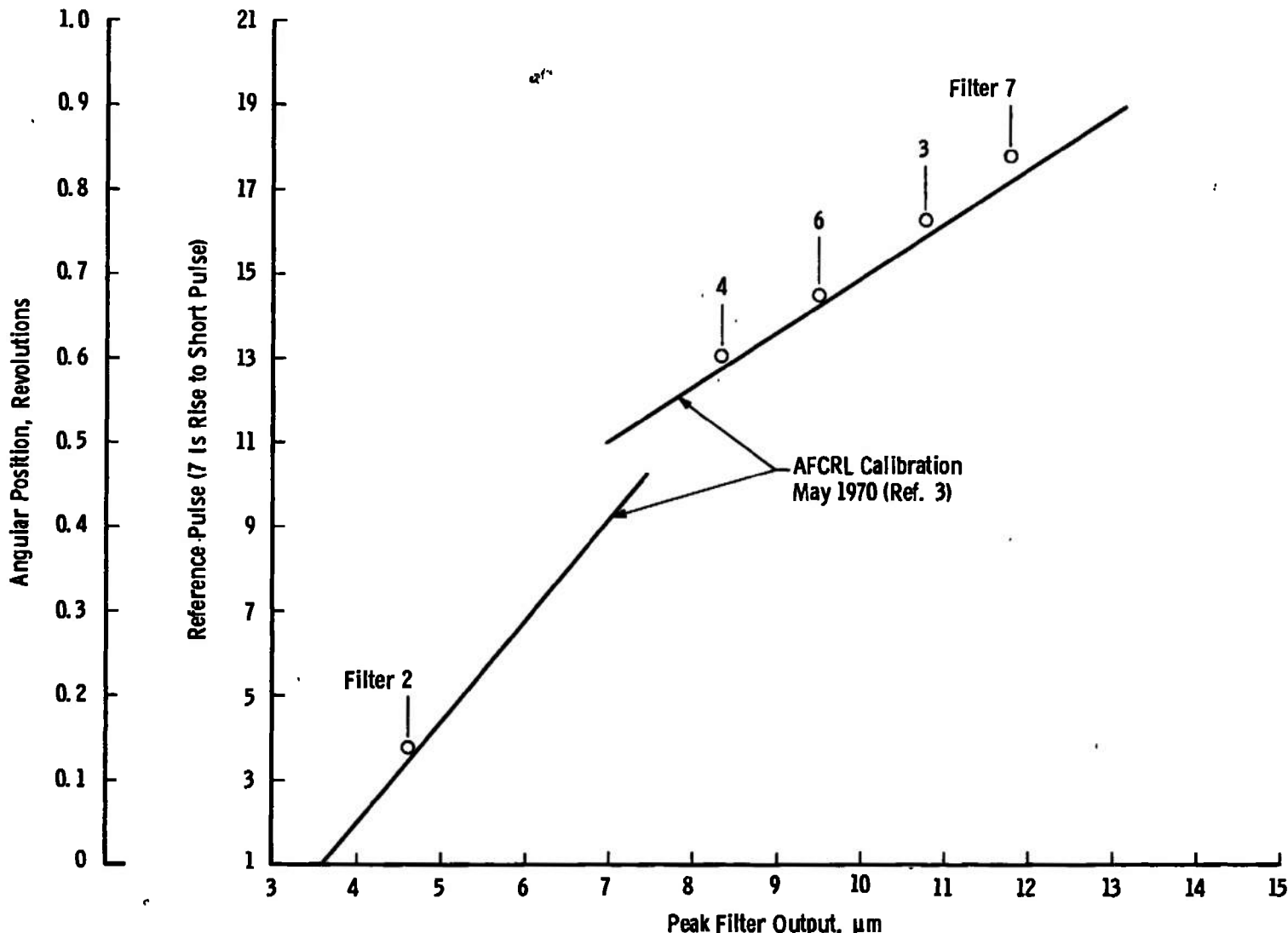


Fig. 12 Wavelength Calibration

**TABLE I**  
**HS-1 ANGULAR RESPONSE**

<u>Distance, eighths of an inch</u>	<u>Polar Angle, deg</u>	<u>HS-1 Gain</u>	<u>V<sub>T</sub></u>	<u>f(V)</u>	<u>f(V) f(V)max</u>
30	7.3	2	0.63	6.30 + 01	7.88 - 03
29	6.8	2	2.30	2.30 + 02	2.88 - 02
28	6.3	1	1.88	3.6 + 03	4.50 - 01
27	5.6	1	2.80	7.4 + 03	9.25 - 01
26	4.9	1	2.95	8.0 + 03	1.00 00
25	4.2	1	2.93	8.0 + 03	1.00 00
24	3.1	1	2.90	7.8 + 03	9.75 - 01
23	2.1	1	2.88	7.8 + 03	9.75 - 01
22	1.05	1	2.84	7.7 + 03	9.63 - 01
21	0.0	1	2.85	7.7 + 03	9.63 - 01
20	-1.0	1	2.83	7.7 + 03	9.63 - 01
19	-2.0	1	2.10	4.45 + 03	5.56 - 01
18	-3.1	2	4.70	4.70 + 02	5.88 - 02
17	-4.2	2	0.83	8.30 + 01	1.04 - 02
16	-5.35	3	1.51	1.51 + 01	1.89 - 03
15	-6.2	3	0.27	2.70 00	3.38 - 04
14	-7.2	4	2.36	2.36 00	2.95 - 04

**TABLE II**  
**HS-1 OFF-AXIS REJECTION**

<u>Polar Angle, deg</u>	<u>Gain</u>	<u>V<sub>T</sub></u>	<u>f(V)</u>	<u>f(V)</u> <u>f(V)max</u>
6. 20	1	4. 10	---	---
6. 25		2. 72	7. 3 + 03	1. 00 00
6. 70		1. 71	3. 0 + 03	4. 11 - 01
7. 11		1. 36	1. 7 + 03	2. 33 - 01
8. 03		0. 99	9. 0 + 02	1. 23 - 01
8. 80		0. 75	5. 5 + 02	7. 53 - 02
9. 60		0. 76	5. 5 + 02	7. 53 - 02
10. 50	↓	0. 68	5. 0 + 02	6. 85 - 02
11. 20	1	0. 42	3. 1 + 02	4. 24 - 02
12. 20	2	1. 93	1. 93 + 02	2. 64 - 02
13. 00		1. 44	1. 44 + 02	1. 97 - 02
13. 90		1. 73	1. 77 + 02	2. 42 - 02
15. 00	↓	0. 49	4. 9 + 01	6. 71 - 03
15. 90	2	0. 44	4. 4 + 01	6. 03 - 03
16. 80	3	3. 84	3. 8 + 01	5. 21 - 03
17. 60		3. 39	3. 4 + 01	4. 66 - 03
18. 50		3. 17	3. 17 + 01	4. 34 - 03
19. 20		3. 01	3. 01 + 01	4. 12 - 03
20. 50		3. 56	3. 56 + 01	4. 87 - 03
21. 20		3. 27	3. 27 + 01	4. 48 - 03
22. 20		1. 98	1. 98 + 01	2. 71 - 03
23. 00		1. 80	1. 80 + 01	2. 47 - 03
24. 70		1. 46	1. 46 + 01	2. 00 - 03
26. 50		1. 16	1. 16 + 01	1. 59 - 03
28. 50		0. 77	7. 7 00	1. 05 - 03
30. 70	↓	0. 51	5. 1 00	6. 99 - 04
32. 80	3	0. 30	3. 0 00	4. 11 - 04
34. 80	4	1. 03	1. 03 00	1. 41 - 04

TABLE III  
WAVELENGTH CALIBRATION DATA

Filter No.	Calibrated Peak of Narrowband Filter, $\mu\text{m}$	Angular Position of Peak Signal, $\mu\text{m}$ revolutions	Angular Position from May 1970 Calibration, revolutions	Apparent Error (+)	Wavelength Error Attributable to Using May 1970 Calibration (+), $\mu\text{m}$
2	4.60	0.139	0.122	0.017(6.1°)	0.14
4	8.35	0.604	0.590	0.014(5.0°)	0.23
6	9.50	0.675	0.663	0.013(4.7°)	0.18
3	10.77	0.765	0.746	0.019(6.8°)	0.30
5	11.30	(no data)	---	---	---
7	11.80	0.840	0.811	0.029(10.4°)	0.45

## UNCLASSIFIED

Security Classification

## DOCUMENT CONTROL DATA - R &amp; D

(Security classification of title, body of abstract and indexing annotation must be entered when the overall report is classified)

1 ORIGINATING ACTIVITY (Corporate author) Arnold Engineering Development Center ARO, Inc., Operating Contractor Arnold Air Force Station, Tennessee 37389		2a. REPORT SECURITY CLASSIFICATION UNCLASSIFIED
		2b. GROUP N/A
3 REPORT TITLE FINAL PREFLIGHT CALIBRATION OF ARPA/AFCRL CVF II SPECTROMETER		
4 DESCRIPTIVE NOTES (Type of report and Inclusive dates) Final Report October 7 to 15, 1970		
5 AUTHOR(S) (First name, middle initial, last name) F. Arnold, ARO, Inc. and T. P. Condron, USAF		
6 REPORT DATE May 1971	7a. TOTAL NO OF PAGES 33	7b. NO OF REFS 4
8a. CONTRACT OR GRANT NO F40600-71-C-0002	9a. ORIGINATOR'S REPORT NUMBER(S) AEDC-TR- 71-72	
8b. PROJECT NO. 0450	9b. OTHER REPORT NO(S) (Any other numbers that may be assigned this report) ARO-VKF-TR-71-36	
c. System 920F		
d. Program Element 62301D		
10 DISTRIBUTION STATEMENT <del>This document may be further distributed by any holder only with specific prior approval of Air Force Cambridge Research Laboratories (CROR), L.G. Hanscom Field, Bedford Massachusetts 01730.</del>		
11 SUPPLEMENTARY NOTES Available in DDC.	12 SPONSORING MILITARY ACTIVITY Air Force Cambridge Research Laboratories (CROR), L.G. Hanscom Field, Bedford, Mass. 01730.	
13 ABSTRACT The final preflight calibration tests of the ARPA/AFCRL CVF II spectroradiometer were performed in the Aerospace Research Chamber (7V). These tests included linearity, absolute responsivity, angular response, frequency response, and wavelength calibration. The measured field of view was 8.4 deg or $1.69 \times 10^{-2}$ sr with an off-axis rejection ratio of $10^{-5}$ at 34 deg off axis. The instrument was linear over most of its range, but displayed nonlinearity for high irradiance levels. Wavelength calibration was found to have not changed significantly from a previous calibration. The absolute responsivity at $6.10 \mu\text{m}$ was found to be $4.7 \times 10^{11} \text{ v/w/cm}^2\text{-}\mu\text{m}$ , and spectral responsivity was calculated based on this value in combination with relative spectral data obtained during a previous test.		
<del>This document may be further distributed by any holder only with specific prior approval of Air Force Cambridge Research Laboratories (CROR), L.G. Hanscom Field, Bedford, Massachusetts 01730.</del>		

**UNCLASSIFIED****Security Classification**

14.  KEY WORDS	LINK A		LINK B		LINK C	
	ROLE	WT	ROLE	WT	ROLE	WT
spectrometers						
environmental tests						
calibration						
performance evaluation						
infrared detectors						
spectral emittance						
reflectance						